AIAA JOURNAL
Vol. 32, No. 4, April 1994

Airfoil Pressure Measurements During Oblique Shock-Wave/Vortex Interaction in a Mach 3 Stream

Iraj M. Kalkhoran* and Pasquale M. Sforza†
Polytechnic University, Brooklyn, New York 11201

An experimental investigation of the interaction between streamwise discrete vortices and oblique shocks formed over a two-dimensional wedge surface was conducted in a Mach 3 blowdown wind tunnel. An instrumented two-dimensional wedge section was placed downstream of a semispan wing so that the trailing tip vortex would arbitrarily interact with the shock wave formed over the wedge surface. The experiments were designed to simulate interaction of streamwise vortices from upstream bodies with shock waves formed over aft surfaces as might be encountered in supersonic flight of aircraft and missiles. The influence of vortex strength and vortex-airfoil vertical separation distance on the interaction was examined. The flowfield generated was found to be highly unsteady, and a substantial change in the pressure distribution on the downstream airfoil was observed. The interaction of a strong vortex with the oblique shock wave over the downstream wedge section resulted in formation of an unsteady detached shock wave upstream of the wedge leading edge. Furthermore, when the vortex approached the wedge leading edge, formation of a detached shock wave occurred further upstream of the section leading edge.

Nomenclature

Cp	=	pressure coefficient, $(p - p_\infty)/q_\infty$
c	=	airfoil chord
h	=	distance between the airfoil leading edge and the vortex-generator tip (Fig. 1)
L	=	characteristic length
M	=	Mach number
p	=	pressure
q	=	dynamic pressure
Re	=	Reynolds number
t	=	time
V	=	velocity
w	=	uncertainty
x, y, z	=	Cartesian coordinates
α	=	vortex-generator angle of attack
Γ	=	circulation
ζ	=	vorticity
ρ	=	density

Subscripts

n	=	normal
t	=	tangential
VG	=	vortex-generator
1	=	condition ahead of the shock
2	=	condition behind the shock
∞	=	freestream

Introduction

INTERACTIONS of concentrated rolled-up vortices with lifting surfaces are known to have practical importance in the operational environment of high-speed aircraft and missiles.[1,2] Vortices created by forebodies or forward lifting surfaces (e.g., wings, canards, and forward fins) of a vehicle operating at angle of attack convect downstream and may interact with aft lifting surfaces or air intake systems leading to aerodynamic heating, dynamic loading, and flow distortions that influence stability and dynamic characteristics of the vehicle. At supersonic speeds, the flowfield generated by such encounters is in general three-dimensional and unsteady with strong compressibility effects due to the presence of shock waves. Under certain operating conditions, vortices encountering abrupt pressure jumps across shock fronts generated by downstream surfaces may suffer distortion that would significantly alter the aerodynamic characteristics of these surfaces. For example, it has been experimentally demonstrated[3-5] that interaction of streamwise vortices with normal shock waves may result in vortex breakdown. The vortex breakdown phenomenon is characterized by a sudden change in structure of the vortex, including the appearance of a stagnation point on the axis, an increase in vortex diameter, and a reduction in circumferential velocity.[6,7]

A simple dimensional analysis of the shock-wave/vortex interaction problem indicates that the governing simulation parameters are Mach number, Reynolds number, a vortex intensity parameter defined by $\Gamma/V_\infty L$, a shock strength parameter defined by ρ_2/ρ_1, the density ratio across the shock, and the shock-wave inclination angle.[8] Depending on the shock-wave inclination angle relative to the freestream direction, two types of interactions are of interest: a normal shock-wave/vortex interaction and an oblique shock-wave/vortex interaction. Fundamental theoretical studies by Hayes[9] demonstrated that the vorticity jump across a shock discontinuity is given by

$$\delta\zeta_n = 0 \tag{1}$$

$$\delta\zeta_t = \boldsymbol{n}\boldsymbol{x}[\nabla_t(\rho V_n)\delta\rho^{-1} - (\rho V_n)^{-1}\boldsymbol{V}_t\cdot\nabla_t\boldsymbol{V}_t\delta(\rho)] \tag{2}$$

where $\boldsymbol{n}$ is the unit vector normal to the discontinuity surface, the subscript t indicates the component of vector quantities tangent to the shock surface, and the velocity vector $\boldsymbol{V}$ for the flowfield is given by

$$\boldsymbol{V} = \boldsymbol{n}V_n + \boldsymbol{V}_t \tag{3}$$

Thus, a streamwise vortex will experience no jump in vorticity across a normal shock, whereas the same vortex will expe-

Presented as Paper 92-2631 at the AIAA 10th Applied Aerodynamics Conference, Palo Alto, CA, June 22-24, 1992; received July 7, 1993; revision received Nov. 8, 1993; accepted for publication Nov. 9, 1993.

*Assistant Professor, Aerospace Engineering Department. Member AIAA.

†Professor and Head, Aerospace Engineering Department. Associate Fellow AIAA.

rience a finite jump in its vorticity when crossing a planar oblique shock front. In practice, however, introduction of a vortex filament in a uniform freestream upstream of an otherwise planar shock will give rise to a locally deformed and curved shock structure leading to a jump in the tangential component of vorticity across the shock as given by Eq. (2) for both normal and oblique shock-wave/vortex interactions.

Previous experimental and numerical studies relevant to the interaction problem have focused on understanding the physics of shock-wave/vortex interaction and development of the vortex breakdown in supersonic flows. Moreover, such studies have mainly concentrated on interaction of streamwise vortices with normal shock waves. To the authors' knowledge, the only systematic study of the oblique shock-wave/vortex interaction problem was reported in Ref. 10 where Copening and Anderson used the three-dimensional Euler equations to study interaction of vortices with oblique shock waves at Mach numbers of 2.28 and 5. They observed no vortex breakdown or appreciable alteration of vortex strength as a result of interactions; however, they reported regions of reversed flow as well as convex-concave shock shape. On the experimental side, Delery et al.[3] carried out a wind-tunnel study of the interaction of streamwise vortices with normal shock waves and reported some shock-induced modifications to both structure and the trajectory of vortices. Moreover, they established a vortex-breakdown criterion as a function of vortex swirl rate and shock intensity for the case of nearly uniform axial velocity distribution in the vortex core. Their results also indicated that interactions in which vortex breakdown occurs lead to negative axial velocity at the vortex axis, a considerable reduction in maximum tangential velocity, and an increase in the radius of the vortex viscous core, which are all characteristics of incompressible vortex breakdown.

Dissipation of streamwise vortices as a result of interaction with normal shock waves in an inlet-type configuration was experimentally investigated by Zatoloka et al.[4] They reported development of a stagnation zone as well as a distorted shock pattern as a result of such encounters. Interactions of vortices with normal shock waves were also experimentally studied by Metwally et al.[5] and Cattafesta et al.,[11] who reported a strong influence of vortex swirl rate and Mach number on the interaction, a vortex breakdown, and an upstream shock propagation. The experimental results of Refs. 5 and 11 suggested a hypothetical supersonic vortex breakdown model consisting of a region of reversed flow as well as a stagnation point downstream of a bulged-forward shock wave. Head-on interaction of tip vortices with a wedge surface in a Mach 3 flow was reported in Ref. 8 where the encounter resulted in formation of a locally detached shock front far upstream of the wedge leading edge. In addition, the distorted vortex structure was reported to form a slip surface separating a subsonic zone from a supersonic region. The aforementioned experimental studies all involve interaction of concentrated streamwise vortices with normal shock waves that have subsonic flow downstream of the interaction. As a result, deceleration of the vortex axial velocity is accomplished in a manner similar to the subsonic vortex breakdown. On the other hand, since supersonic flow is maintained downstream of an oblique shock, a vortex breakdown resembling a subsonic case during oblique shock-wave/vortex encounter will only be possible if a normal shock develops as a result of the encounter.

The present experimental investigation was designed to study the interaction of streamwise vortices of various strength with oblique shock waves and their effect on the aerodynamic characteristics of the shock-generating surface. Moreover, the experiment was designed to represent an interaction problem similar to that found in practice.

Experimental Setup, Test Conditions, and Instrumentation

The experimental study was conducted in the Mach 3 blowdown wind tunnel at Polytechnic University.[12] The wind tunnel has a 25.4 × 25.4 cm^2 (10 × 10 in.^{2}) test section and is capable of producing flow with a nominal Mach number of 3.1 and Reynolds numbers in the range of 6 × 10^7 to 16 × 10^7 per meter (16 × 10^6 to 48 × 10^6 per foot). A schematic of the experimental arrangement is shown in Fig. 1. A tip vortex is generated by an unswept semispan slender wing section (Fig. 2) with a thickness of 10.6%, a chord length of 7.62 cm (3 in.), and a semispan of 11.94 cm (4.7 in.). The vortex-generator wing was mounted on the test section ceiling along the tunnel centerline and extended vertically downward (Fig. 1). The vortex-generator wing could be set at different angles of attack so that vortices of various strengths could be generated. The downstream interacting airfoil (Fig. 3) was a two-dimensional wedge section with a chord length of 3.81 cm (1.5 in.) that extended the entire width of the test section. The section had a wedge angle of 27 deg and was equipped with 18 pressure taps in 3 spanwise locations at $Y/c = -0.13$, 0.0, and 0.13 ($Y = 0$ is the middle of the semispan wing) and

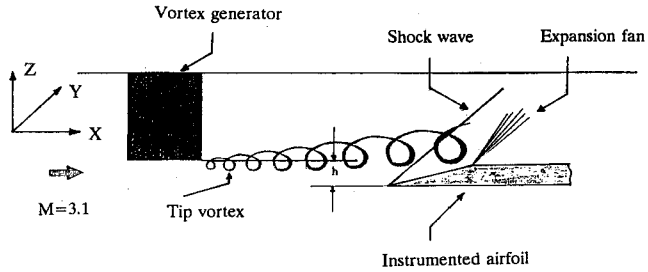

Fig. 1 Schematic of the oblique shock-wave/vortex interaction experiments.

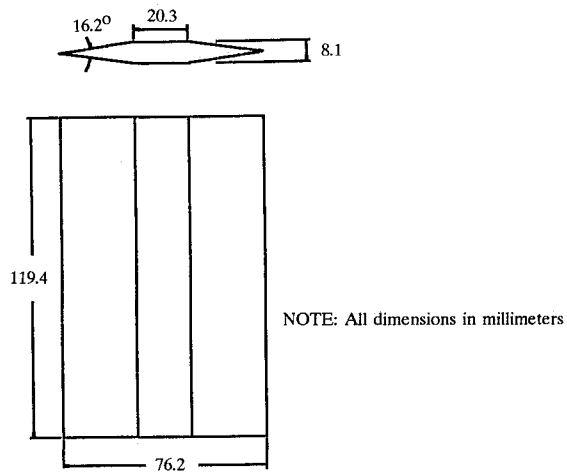

Fig. 2 Geometry of the vortex-generator section.

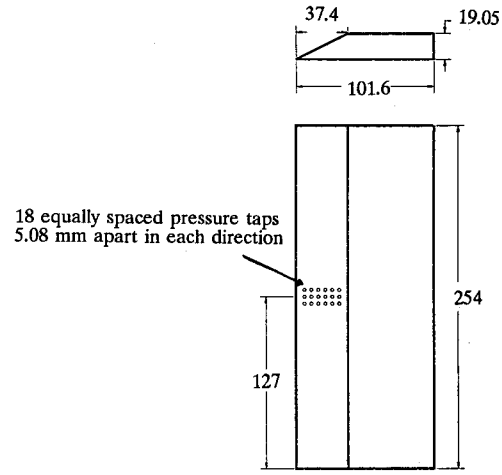

Fig. 3 Geometry of the 27-deg shock-generator section.

6 equally spaced chordwise locations from $X/c = 0.13$ to 0.80. The test airfoil was placed approximately 15.7 cm (6.2 in.) or about two vortex-generator chords downstream of the vortex generator and was capable of being traversed in the vertical direction so that interactions at various vortex heights over the airfoil could be studied.

For the current study, the test section Mach number was 3.1, and the wind-tunnel stagnation pressure and temperature were 1.2 MPa (170 psia) and ambient (298 K), respectively, resulting in a unit Reynolds number of approximately 8.4×10^7 per meter. The results of a conventional uncertainty analysis indicate that, for the range of data reported in this paper, the typical ranges of values for the uncertainty in the principle test variables are $w_M = 0.009$–0.022 and $w_{Cp} = 0.014$–0.035. Typical wind-tunnel running times were 3 s, and pressure measurements were performed at a sampling frequency of 250 Hz for a period of 2 s. Visualization of the flowfield was accomplished by the shadowgraph method using sparks providing microsecond-range exposure times. Multiple spark shadowgraphs of the flowfield during a typical run were used to detect transient flow behavior.

Experimental Results and Discussion—Airfoil Calibration

Airfoil calibration experiments aimed at establishing baseline undisturbed pressure distribution data were conducted before the interaction studies. Figure 4 illustrates the chordwise pressure coefficient distribution for three spanwise stations. These traces were obtained by time averaging the pressure transducer outputs during the steady-state portion of wind-tunnel operation. In general, the measured pressure distribution compared favorably with theoretical prediction of $Cp = 0.689$, and repeatability runs showed consistency from one run to the next.

Shock-Wave/Vortex Interaction Results

Shock-wave/vortex interaction experiments were conducted using the wing tip vortex generated by placing the vortex-generator wing at 5, 7.5, or 10 deg angle of attack. The downstream interacting airfoil was kept at zero angle of attack for all cases, whereas the effect of vortex-airfoil vertical separation distance was examined by traversing the downstream wedge section up or down. Repeatability runs (generally three runs per configuration) were conducted to verify the consistency of experimental data from one run to the next.

Shock-wave/vortex interaction experiments with vortex-airfoil vertical separation distances of $h/c = 0.4$, 0.23, 0.067, -0.1, and -0.267 were examined (Fig. 1). It should be noted that the quantity h in the nondimensional separation distance parameter h/c is a reference geometric parameter defined by the vertical distance between the vortex-generator tip and the airfoil leading edge and does not represent the actual vortex height relative to the airfoil leading edge. Furthermore, a negative value for vertical separation distance represents situations in which the vortex-generator tip is below the leading edge of the downstream wedge section. Extensive shadowgraphs of the flowfield taken during the encounter indicated that separation distances represented by $h/c = 0.4$, 0.23, and 0.067 correspond to situations in which the vortex passes above the wedge section creating an oblique shock-wave/vortex interaction. On the other hand, the cases represented by $h/c = -0.1$ and -0.267 correspond to cases in which the core region of the tip vortex impinges on the leading edge of the wedge surface. The interaction experiments for these closer encounters were found to be highly unsteady with a vertical oscillating movement of the vortex core leading to unsteady head-on interactions of the vortex with the wedge leading edge.

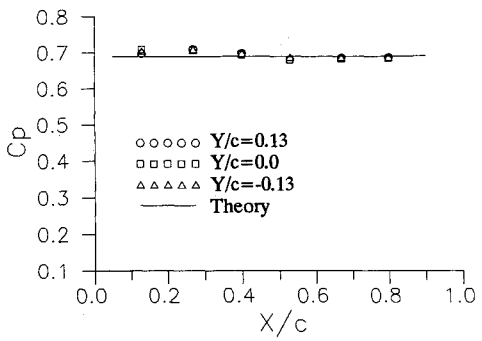

Fig. 4 Baseline wedge pressure distribution.

Results for the Weak Interaction

The interaction experiments were initiated by placing the vortex-generator wing at an angle of attack of 5 deg to generate a relatively weak vortex. Figure 5 shows a typical spark shadowgraph of the flowfield for the case of $h/c = 0.40$ and $\alpha_{VG} = 5$ deg. In that picture, the flow is from left to right, and the vortex generator and the wedge section may be seen at the upper left and lower right portions of the shadow photograph, respectively. The picture clearly indicates a concentrated tip vortex with a sensible rollup convecting downstream and intersecting the oblique shock wave formed by the wedge. The study of shadowgraphs for the interaction of weak vortices with the shock wave indicated only a slight modification of the shock wave as a result of the encounter within the viewing area, which includes the entire airfoil chord.

Time-averaged chordwise and spanwise wedge surface pressure distributions, in terms of Cp, for three vortex-wedge separation distances are compared with the baseline pressure distribution in Fig. 6. These trends indicate that the vortex influence on the airfoil pressure distribution is a strong function of both vortex-airfoil vertical separation distance as well as spanwise location on the airfoil. These figures suggest that closer to the wedge leading edge the vortex influence is limited to the region $Y/c > 0$ for all vortex core heights. Further downstream the vortex is seen to influence a larger spanwise portion of the wedge surface, indicating the possibility of a growth in vortex size as a result of the interaction. For the case in which the vortex was furthest away from the airfoil surface, i.e., $h/c = 0.4$ (Fig. 6a), the vortex influence on the wedge pressure distribution may be seen to be more uniform along the airfoil chord, whereas, for the closest encounter represented by $h/c = -0.267$ (Fig. 6c), the vortex influence is seen to be a stronger function of the chordwise location. On the other hand, Fig. 6b, which represents an intermediate vortex-airfoil separation distance, shows that for $Y/c = 0$ and -0.13 the vortex influence on the wedge surface pressure distribution continues to increase up to approximately the midchord location, whereas beyond $X/c = 0.53$ the vortex influence on the airfoil pressure distribution tends to diminish.

For the closest encounter represented by $h/c = -0.267$, the shadowgraphs of the flowfield indicate a head-on inter-

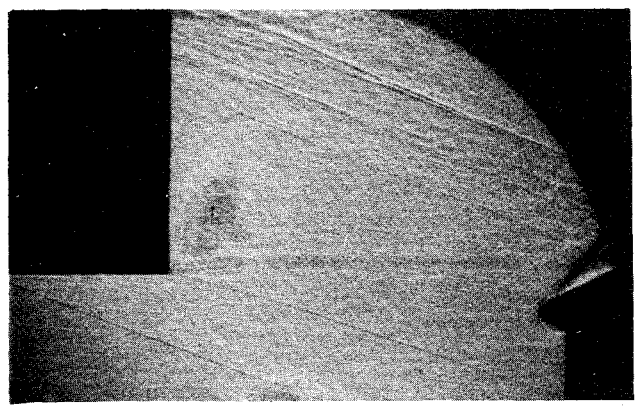

Fig. 5 Shadowgraph of the flowfield generated during the weak interaction, $\alpha_{VG} = 5$ deg, $h/C = 0.40$.

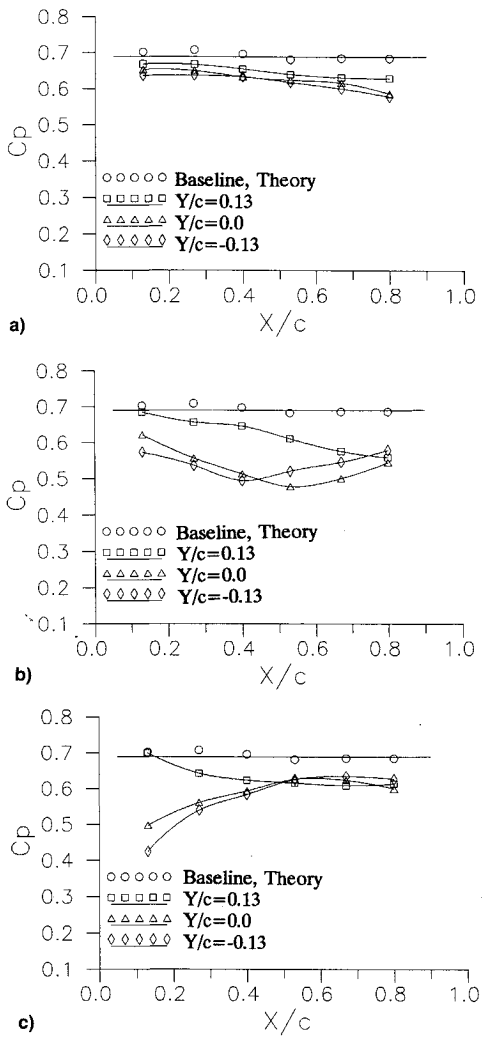

Fig. 6 Wedge pressure coefficient distribution during the interaction for α_{VG} = 5 deg: a) h/C = 0.40, b) h/C = 0.067, and c) h/C = −0.267.

action of the vortex core with the wedge leading edge. The wedge surface pressure distribution for this case is shown in Fig. 6c and indicates that the most pronounced vortex influence is near the airfoil leading edge, and a progressively reduced effect on the wedge pressure distribution is seen at distances further downstream. Shadowgraphs of the flowfield taken during the weak encounters also indicate that the flowfield downstream of the interaction is supersonic, limiting the region of the flowfield affected by the interaction to the Mach cone originating at the intersection of the vortex and the shock wave. Thus vortex influence on the wedge surface pressure distribution is moved closer to the leading edge as the vortex-airfoil vertical separation distance decreases.

Results for the Strong Interaction

Interaction experiments incorporating stronger vortices were found to have similar trends to those of weak interaction results discussed earlier but with a more pronounced change in the wedge pressure distribution. Typical wedge pressure distributions for the strong interactions are shown in Figs. 7 and 8, corresponding to the vortex-generator angles of 7.5 and 10 deg, respectively. Again, similar to the weak interaction results, for the vortex-wedge vertical separation of h/c = 0.067 (Figs. 7a and 8a), a progressively increased vortex influence on the airfoil pressure distribution up to approximately the midchord location for all spanwise stations is seen. The spanwise extent of the vortex influence may also be seen to be more pronounced for $Y/c > 0$ near the airfoil leading edge, whereas further downstream the vortex influence expands in the spanwise direction to include Y/c = 0.13.

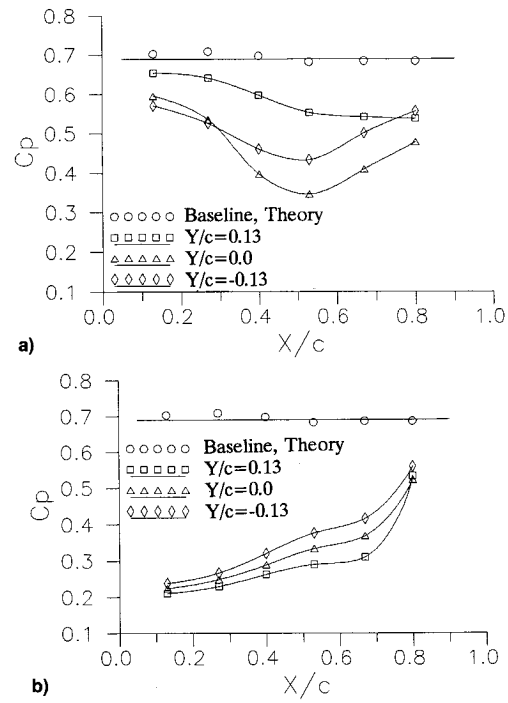

Fig. 7 Wedge pressure coefficient distribution during the interaction for α_{VG} = 7.5 deg: a) h/C = 0.067 and b) h/C = −0.267.

Interaction results for the closer encounters represented by h/c = −0.10 and −0.267 (Figs. 7b and 8c) resulted in the most significant alteration of the airfoil pressure distribution near the airfoil leading edge, whereas, similar to the weaker interactions, the spanwise extent of the vortex influence for these cases includes all stations with the results for Y/c = 0.13 on the same order as Y/c = 0 and −0.13. These trends suggest that vortex influence on the wedge pressure distribution moves closer to the leading edge as the vortex airfoil separation distance decreases. This may be seen by comparing the chordwise pressure distributions at Y/c = 0.13 in Figs. 8a and 8b for h/c = 0.067 and −0.10, respectively. Figure 8a indicates a favorable chordwise pressure gradient up to X/c = 0.53, whereas Fig. 8b indicates, for the case represented by h/c = −0.10, that vortex-induced suction is terminated at X/c = 0.26.

Spark shadowgraphs of the flowfield during the interaction process may be used to gain further insight into the complex flowfield generated by the shock-wave/vortex interactions. Figure 9 illustrates sequential spark shadowgraphs of the flowfield for one test case of h/c = 0.40 and α_{VG} = 10 deg. This case represents a situation in which the vortex passes over the wedge surface and intersects the oblique shock wave, a classic example of an oblique shock-wave/vortex interaction. Figure 9a indicates formation of a compression wave just downstream of the oblique shock, whereas Fig. 9b, taken a distinct time later, shows formation of a detached shock wave with its vertex situated at the vortex center and above the airfoil leading edge. The aforementioned picture also clearly indicates a growth of the vortex size behind the detached shock wave, a situation similar to that found in vortex breakdown phenomena. A closer examination of Fig. 9b reveals a strong shock curvature at the apex with the leading portion of the shock being normal to the axial flow direction. Consequently, the flow represents a situation in which an oblique shock-wave/vortex interaction leads to a normal shock-wave/vortex interaction with a subsonic flow downstream of the detached shock. Such observation suggests an important aspect of supersonic vortex breakdown that may be expected during oblique shock-wave/vortex interaction, i.e., the presence of a local subsonic region. To the authors' knowledge, a vortex distortion as a result of oblique shock-wave/vortex

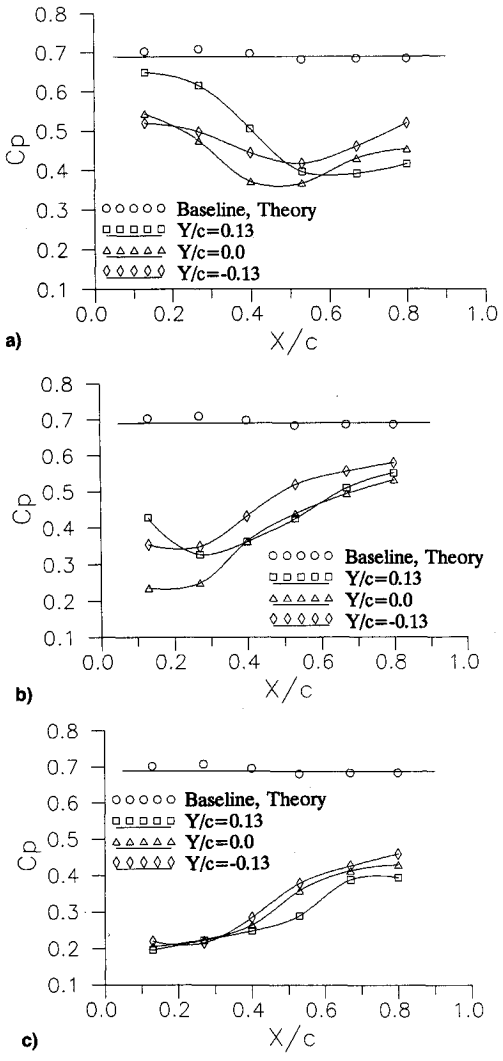

Fig. 8 Wedge pressure coefficient distribution during the interaction for α_{VG} = 10 deg: a) h/C = 0.067, b) h/C = −0.10, and c) h/C = −0.267.

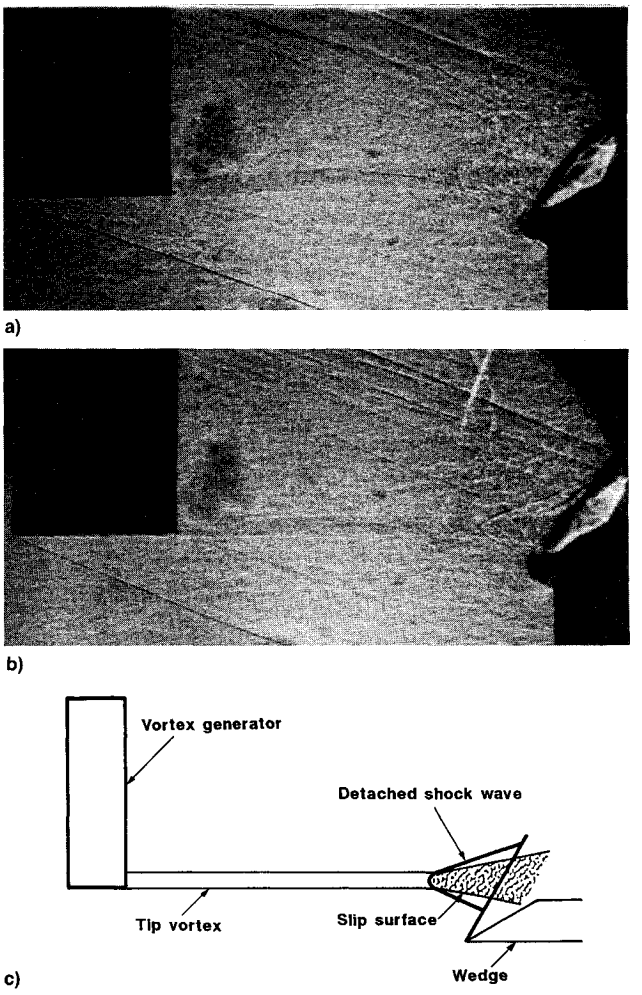

Fig. 9 Sequential shadowgraphs of the flowfield generated during the oblique shock-wave/vortex interaction for α_{VG} = 10 deg, h/C = 0.40: a) $t = t1$, b) $t = t2$, and c) interpretation of the observed flowfield in Fig. 9b.

interaction similar to that seen in Fig. 9b has not been reported in the past. An interpretation of the observed flowfield in Fig. 9b based on the supersonic vortex distortion model reported in Ref. 8 is shown in Fig. 9c. Similar results were observed for a vortex-wedge vertical separation distance of h/c = 0.067. Repeatability runs, however, indicated formation of different size detached waves and the flowfield was found to be highly unsteady.

The flowfield was found to depend strongly on the vertical position of the vortices with respect to the leading edge of the interacting surface, resulting in a variety of unsteady interactions. An example of such a case may be seen in Fig. 10 where sequential spark shadow photographs for h/c = −0.10 are shown. Figure 10a shows the vortex intersecting the shock wave slightly above the wedge leading edge, resulting in formation of a small "bubble-type" shock wave similar to that reported in Ref. 11. At a later time the vortex seems to be deflected slightly downward, leading to what is thought to be a head-on collision of the vortex core and the airfoil leading edge. As a result, a detached shock wave forms some distance upstream of the wedge leading edge. Further reduction of the vortex-airfoil separation distance to h/c = −0.267 resulted in a more pronounced upstream movement of the detached shock followed by a more rapid growth of the vortex core size downstream of the detached shock wave. Further examples of the head-on interaction of tip vortices with the wedge surface may be found in Ref. 8. In general, the flowfield generated by this case was also found to be unsteady

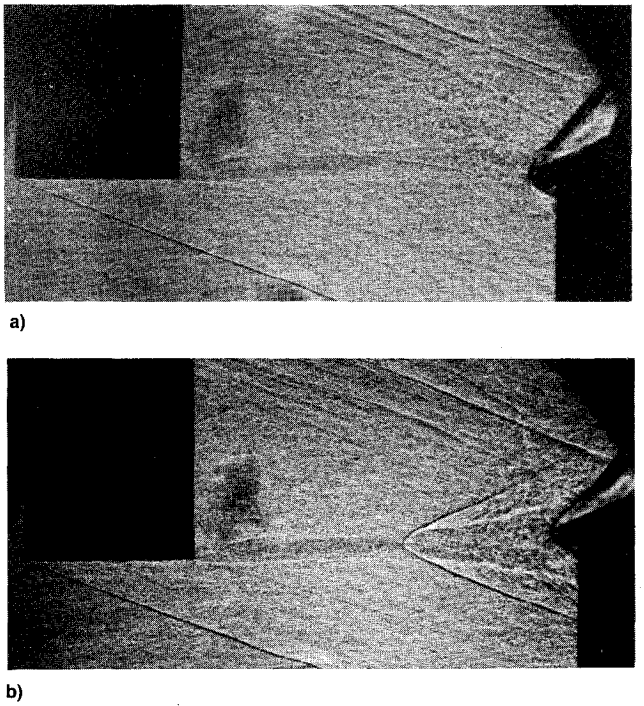

Fig. 10 Sequential shadowgraphs of the flowfield generated during the head-on interaction of the tip vortex and the wedge leading edge for α_{VG} = 10 deg, h/C = −0.10: a) $t = t1$ and b) $t = t2$.

with relatively large amplitude wedge surface pressure fluctuations.

In summary, results of the experimental study showed significant sensitivity of the flowfield to the vertical separation between the vortex and the wedge leading edge. Extensive shadowgraph studies taken during the encounters indicate that a head-on collision of the vortex and the wedge leading edge results in formation of detached vortex-distortion shocks. It is postulated that formation of such shock waves are a result of vortex core Mach number distribution and inability of the wedge to support an attached shock wave. A locally detached shock wave will form in front of the actual wedge leading edge if, for example, the locally induced flow angularity is sufficiently high. The leading portion of this locally detached shock wave will be a normal shock with a substantial pressure jump across it, and this is assumed to be responsible for the vortex distortion seen in Fig. 10b. Furthermore, the subsonic region just downstream of the normal portion of the locally detached shock wave will then be responsible for upstream propagation of disturbances created by the vortex distortion that moves the shock wave far upstream of the wedge leading edge, thus the name "vortex distortion shock."

Conclusions

Experimental studies on the interaction of streamwise vortices with oblique shock waves in a supersonic stream were conducted. The shadowgraphs taken during the interaction of relatively weak vortices with two-dimensional oblique shock waves did not reveal significant alteration of the flowfield downstream of the shock wave. On the other hand, the airfoil pressure measurements during the weak interaction indicated a sensible alteration of the airfoil pressure distribution during the encounter. Stronger tip vortices were found to lead to unsteady formation of detached shock waves far upstream of the wedge leading edge along with a substantial vortex-induced influence on the pressure distribution on the interacting airfoil. The flowfield generated by the interaction was found to be quite sensitive to vortex strength and proximity of the vortex core to the wedge leading edge with the most pronounced effect occurring during the head-on interaction of the vortex core and the wedge leading edge.

Acknowledgments

The first author was partially supported by the Air Force Office of Scientific Research (Grant F49620-93-1-0009) and NASA Lewis Research Center (Grant NAG 3-1378). The assistance provided by Lester Orlick and Frank Wang is acknowledged with appreciation.

References

[1]Dillenius, M. F. E., and Perkins, S. C., "Survey on Nonlinear Effects," *Special Course on Missile Aerodynamics*, AGARD-R-754, April 1988.

[2]Mendenhall, M. R., and Nielson, J. N., "Effect of Symmetrical Vortex Shedding on the Longitudinal Aerodynamic Characteristics of Wing-Body-Tail Combinations," NASA CR-2473, Jan. 1975.

[3]Delery, J., Horowitz, E., Leuchter, O., and Solignac, J. L., "Fundamental Studies on Vortex Flows," *LaRecherche Aerospatiale* (English ed.) (ISSN 0379-380X), No. 2, 1984, pp. 1–24.

[4]Zatoloka, V., Ivanyushkin, A. K., and Nikolayev, A. V., "Interference of Vortexes with Shocks in Airscoops. Dissipation of Vortexes," *Fluid Mechanics, Soviet Research*, Vol. 7, No. 4, 1978, pp. 153–158.

[5]Metwally, O., Settles, G., and Horstman, C., "An Experimental Study of Shock Wave/Vortex Interaction," AIAA Paper 89-0082, Jan. 1989.

[6]Leibovich, S., "Vortex Stability and Breakdown: Survey and Extension," *AIAA Journal*, Vol. 22, No. 9, 1983, pp. 1192–1206.

[7]Benjamin, T. B., "Theory of the Vortex Breakdown Phenomenon," *Journal of Fluid Mechanics*, Vol. 14, Dec. 1962, pp. 593–629.

[8]Kalkhoran, I. M., "Vortex Distortion During Vortex-Surface Interaction in a Mach 3 Stream," *AIAA Journal*, Vol. 32, No. 1, 1994, pp. 123–129; also AIAA Paper 93-0761, Jan. 1993.

[9]Hayes, W. D., "The Vorticity Jump Across a Gasdynamic Discontinuity," *Journal of Fluid Mechanics*, Vol. 2, Aug. 1957, pp. 595–600.

[10]Copening, G., and Anderson, J., "Numerical Solutions to Three-Dimensional Shock Wave/Vortex Interaction at Hypersonic Speeds," AIAA Paper 89-0674, Jan. 1989.

[11]Cattafesta, L. N., and Settles, G. S., "Experiments on Shock/Vortex Interaction," AIAA Paper 92-0315, Jan. 1992.

[12]Kalkhoran, I. M., and Sforza, P. M., "Operation and Calibration of Mach 3 Wind Tunnel in the Polytechnic Aerodynamics Laboratory," Polytechnic Univ., Dept. of Aerospace Engineering, POLY AE Rept. 90-3, Brooklyn, NY, Oct. 1990.